Preparation of highly dispersed Mn–Ce mixed metal oxides supported on the nitric vapour functionalised CNTs for low-temperature NO reduction with NH_3

Xin Lv, Yi Zheng ✉

Institute of Chemistry and Environmental Engineering, Shanghai Institute of Technology, Shanghai 200444, People's Republic of China
✉ *E-mail: skyerl123@163.com*

Published in Micro & Nano Letters; Received on 22nd September 2016; Revised on 4th January 2017; Accepted on 17th January 2017

Highly dispersed Mn–Ce mixed metal oxide catalysts supported on the nitric vapour functionalised carbon nanotubes (CNTs) were synthesised by a polyol process for the low-temperature NO reduction with NH_3. The obtained samples possessed high Mn^{4+}/Mn and O_α/$O_\alpha + O_\beta$ ratios and exhibited 90–100% NO conversion at 180–240°C.

1. Introduction: Selective catalytic reduction (SCR) is considered as one of the optimum clean technology for reduction of the NO_x from stationary sources. V_2O_5–WO_3/TiO_2 is usually used as the commercial catalyst for the NH_3-SCR of NO_x [1, 2]. However, some disadvantages exist, such as catalysts should be located downstream of the de-sulphurised and electrostatic precipitators, and the flue gas temperature at this point is usually below 200°C [3]. Therefore, it is necessary to develop highly active low-temperature (<200°C) catalysts.

Recently, Mn-based catalysts, which are famous for the novel chemical and physical properties, have developed for low-temperature SCR of NO with NH_3. However, the low-temperature SCR activity of single component needs to be improved [4, 5]. Complex metal oxides are concerned, which selectivity of N_2 and active window can be changed [6]. The MnO_x–CeO_x binary metal oxides catalysts were possessed of desirable SCR activity, recently, such as MnO_x–CeO_x/TiO_2 [7], MnO_x–CeO_x catalysts [8], Mn–CeO_x/TiO_2 carbon nanotubes (CNTs) [9]. Moreover, CNTs with unique one-dimensional tubular, electronic, physical and chemical characteristics get more and more attention as support materials of the catalysts. In particular, the CNT-based catalysts are not poisoned, and the CNTs are good sorbents of ammonia and nitric oxides [10, 11]. As we know, CNTs have a hydrophobic surface [12]. So it is difficult to uniformly disperse the MnO_x and CeO_x on the CNTs. Herein, we hope to improve the dispersity of the active components by the surface modification of CNTs. The liquid oxidation using vigorous oxidants such as nitric acid or nitric acid and sulphuric acid mixture to remove amorphous carbon and impurities is often recognised as the efficient method [13]. However, it pollutes the environment and damages the essential nanotubes structure and it is difficult to remove the oxidant solution through tedious washing. Recently, we found that functionalisation with HNO_3 vapour can afford surface oxygen functional groups (C=O, –COOH and –OH), which can eliminate agglomerates and serve as the adsorption sites for reducing agents, and enhance the loading efficiency of the metal phase [14–18]. Therefore, the oxygen-containing functional groups are in favour of the enhancement of NH_3-SCR activity. In addition, the application of the HNO_3 vapour treatment is more advantageous by avoiding the tedious filtration and washing. So we first oxidise CNTs via nitric acid vapour to improve the hydrophobic nature in solvents for the SCR catalysts. The catalyst is prepared by a polyol process. Meanwhile, we found non-covalently associating CNTs with polyvinyl pyrrolidone (PVP) can solubilise CNTs in ethylene glycol solution. The CNTs with PVP can uniformly disperse in the ethylene glycol solution. The Mn^{4+} and Ce^{3+} ions are attached to the composites of CNTs and PVP though reflux. We can obtain the catalysts Mn–Ce/CNTs after calcination. The morphology, structural properties as well as the catalytic performance of catalysts were investigated.

2. Experimental

2.1. Catalyst preparation: Pristine multi-walled CNTs (1 g) with 40–60 nm in diameter were loaded on the porous SiO_2 griddle of glass sand crucible, and placed into a 100 ml Teflon-vessel, and 10 ml HNO_3 was previously added to the bottom of the vessel. The vessel was sealed, and then placed into the autoclave. Subsequently, the autoclave was moved to the oven at the temperature of 180°C. After 5 h of operation, took the functionalised CNTs out of the vessel when the autoclave was cool to the room temperature. Then, the CNTs were separated by filtration, washed several times with distilled water and ethanol. Next, the samples were dried at 70°C overnight.

The supported catalysts were synthesised by the polyol process. Manganese acetate and cerium nitrate with different mole ratios and the functionalised CNTs were mixed and dispersed in 100 ml of ethylene glycol upon ultrasonic vibration for 2 h. The mixed solution was refluxed under continuous stirring at 140°C for 10 h. After that, the solution was filtered and washed repeatedly with distilled water and ethanol, and dried at 70°C for 12 h. Finally, the sample was calcined at 400°C for 2 h in N_2 atmosphere. The obtained catalysts are denoted as Mn(y)–Ce/VF-CNTs, where y represents the molar ratio of Mn/(Mn + Ce).

For comparison, the primitive CNTs are oxidised by nitric acid solution. Then the catalyst with optimum Mn/(Mn + Ce) was prepared by an impregnation method. The catalyst synthesised by this way was denoted as Mn–Ce/SF-CNTs. In the typical synthesis, the primitive CNTs were impregnated with a mixed solution of cerium nitrate and manganese acetate. After that the sample was dried at 70°C and calcined at 400°C for 2 h in N_2 atmosphere. The catalyst synthesised by this way was denoted as Mn–Ce/p-CNTs.

2.2. Catalyst characterisation: The power X-ray diffraction (XRD) was performed on a DX-9BG X-ray diffractometer with Cu-K_α (40 kV, 40 mA) radiation. The XRD data were recorded in range of $5° < 2\theta < 80°$. The X-ray photoelectron spectroscopy (XPS) results were obtained using an AXIS Ultra DLD system from Kratos with Al-K_α radiation as X-ray source for radiation. The transmission electron microscopy (TEM) observation was carried out on a JEOL JEM-200CX system. Field emission scanning electron microscopy (FESEM) image was obtained by Nova NanoSEM 230 SUPRA 55 SAPPHIRE instrument equipped an

X-ray probe with 10 keV primary electron energy and about 127 eV energy resolution in the Mn (K_α) peak.

2.3. Catalyst tests: The NH_3-SCR activity measurements are performed in a fixed-bed reactor at 100–300°C and the following reaction condition is $NO = NH_3 = 500$ ppm, 5% O_2, N_2 balance and the gas hourly space velocity of 20,000 h^{-1}. The concentration of NO in the feed gases and the excurrent steams were measured by a KM9106 flue gas analyser. NO conversion was calculated as follows

$$\text{NO conversion}(\%) = \frac{[\text{NO}]_{\text{in}} - [\text{NO}]_{\text{out}}}{[\text{NO}]_{\text{in}}} \times 100\%$$

$$N_2 \text{ selectivity}(\%) = \frac{[\text{N}_2]}{[\text{NO}_x]_{\text{in}} - [\text{NO}_x]_{\text{out}}} \times 100\%$$

3. Results and discussion

3.1. TEM and XRD: Fig. 1 shows the micro-morphology of the samples and the dispersion of the metal oxides on the functioned CNTs were investigated by TEM and SEM. From Fig. 1*a*, many metal oxides nanoparticles were anchored on the surface of CNTs. As shown in Fig. 1*b*, there were no obvious agglomeration of metal oxide particles and the particle size was uniform. To further demonstrate the elemental distribution in the catalysts, the elements mapping was listed in Figs. 1*c–f*. The bright spots in Figs. 1*c–f* indicate the presence of elements C, O, Ce and Mn, respectively. Moreover, the mapping shapes of various elements imply the catalyst has uniform distribution of metal oxides.

The XRD patterns of samples are shown in Fig. 2. The diffraction peaks around 26.2°, 42.86°, 53.9°, 77.3° are ascribed to the characteristic reflections of CNTs [19]. From Fig. 2, it is observed that the diffraction peaks of manganese oxides and cerium oxides are very weak and broad over the Mn–Ce/VF-CNTs catalysts. No obvious peaks ascribed to crystalline phase of manganese oxides or cerium oxides could be observed even at a high loading, which suggested that Mn–Ce mixed oxides dispersed well on the HNO_3 vapour functionalised CNTs. Based on the XRD results above, it can be concluded that the manganese oxides and cerium oxides have poor crystallinity and the metal oxides can be homogeneously dispersed in the Mn–Ce/VF-CNTs catalysts.

3.2. BET: The Brunauer-Emmett-Teller (BET) surface area, pore volume and pore size of the catalysts can be obtained by N_2 adsorption–desorption. As shown in Table 1, functioned CNTs by acid vapour obtained an increase in specific surface area and pore volume owing to the opened tips of CNTs, which is beneficial for the SCR activity. It can be distinguished from Table 1 that surface areas and pore volumes of the Mn–Ce/VF-CNTs catalysts are higher and larger than the catalysts prepared by the other way. It may be a result of the better dispersion of the Mn–Ce/VF-CNTs and the inside channel of CNTs would not be blocked. The results are in good consistency with the TEM study. In general, the high specific surface area and porous structures could provide ideal adsorptive and reactive centres for the reactants, which could be useful in the NH_3-SCR reaction.

3.3. X-ray photoelectron spectroscopy: The XPS measurements were carried out to provide the information about the metal oxidation states of the elements. The obtained XPS spectra of Mn 2p, Ce 3d, C 1s and O 1s are shown in Fig. 3, and the corresponding surface atomic mole ratios and compositions are summarised in Table 2.

Fig. 3*a* presents the C 1s spectra of the catalysts. By performing peak-fitting deconvolutions, the C 1s spectra of the CNTs functioned by HNO_3 vapours could be separated into carbon sp^2 (C=C, 284.8 eV), sp^3 (C-C, 285.1 eV), epoxy/hydroxyls (C–O, 286.2 eV) and carboxylates (O–C=O, 288.9 eV) [20]. Therefore, the results indicate that there are large amounts of acidic groups after HNO_3 vapour treatment. These oxygen-containing groups could provide active sites for MnO_x–CeO_x particles over the Mn–Ce/VF-CNTs catalysts and enhance the ability of the CNTs to support metal oxides, which are beneficial for the NH_3-SCR activity.

The Mn $2p_{2/3}$ spectrum can be divided into three characteristic peaks, which can be assigned to Mn^{2+} (640.4 eV), Mn^{3+} (642.2 eV) and Mn^{4+} (644.5 eV) by performing peak-fitting deconvolution, respectively [21, 22]. According to the XPS results, the concentration of Mn and Mn^{4+} on the Mn–Ce/VF-CNTs is 88.97% and higher than that on the Mn–Ce/p-CNTs catalysts. Previous studies have demonstrated that the manganese species with higher oxidation state were preferable for redox properties in the NH_3-SCR reaction at low temperature [23]. Moreover, it has been found that a high Mn^{4+} ratio would promote the reduction of NO to N_2, which is favourable to improve the electron transfer and enhance the SCR activity [21].

The Ce 3d spectrum in Fig. 3*d* was deconvoluted by the curve-fitting procedure. The peaks denoted as u_0 (879.9 eV), u (882.63 eV), u_2 (889.11 eV), u_3 (898.31 eV), and v_0 (899 eV), v (901.28 eV), v_2 (907.59 eV), v_3 (916.69 eV) were assigned to the Ce^{4+} species, while u_1 (885.3 eV) and v_1 (903.67 eV) were indexed to Ce^{3+} species, which imply the coexistence of Ce^{4+} and Ce^{3+} species [22]. As is well documented in the literature, the presence of partial Ce^{3+} species could create the oxygen vacancies and unsaturated chemical bonds on the catalyst surface, which could be beneficial for the activity of the active oxygen species and hence

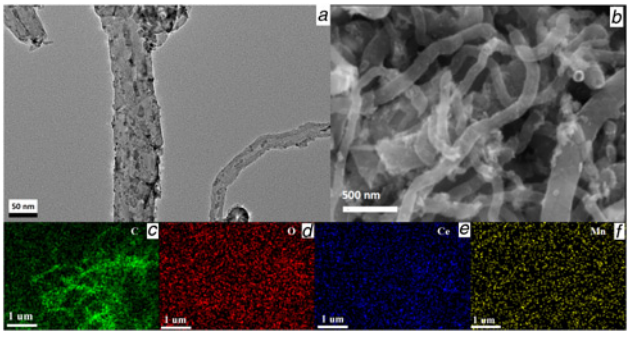

Fig. 1 *Micro-morphology of the samples*
a TEM image
b FESEM image
c–f Elements mapping images of Mn–Ce/VF-CNTs catalysts

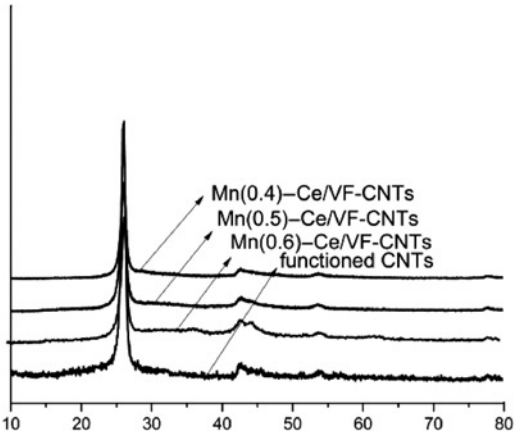

Fig. 2 *XRD patterns of the Mn–Ce/VF-CNTs catalysts*

doi: 10.1049/mnl.2016.0593

Table 1 Surface area and pore characterisation of samples

Samples	BET surface area, $m^2\ g^{-1}$	Pore volume, $cm^3\ g^{-1}$	Pore size, nm
Raw-CNTs	116.4	0.54	18.56
VF-CNTs	146.9	0.65	18.43
Mn–Ce(0.5)/ VF-CNTs	195.3	0.83	16.71
Mn–Ce(0.5)/ p-CNTs	155.4	0.71	14.91

Table 2 Corresponding surface atomic mole ratios and compositions of the samples

Catalysts	C, %	Mn, %	Ce, %	O, %	Mn^{4+}, %	O_α, %	Ce^{3+}, %
Mn–Ce(0.5)/ VF-CNTs	88.8	1.0	0.12	10.0	58.7	60.1	16.3
Mn–Ce(0.5)/ p-CNTs	90.3	0.89	0.38	7.9	46.7	51.3	10.9

increase the SCR activity and N_2 selectivity [21]. As shown in Table 2, the ratio of $Ce^{3+}/(Ce^{4+}+Ce^{3+})$ for Mn–Ce/ VF-CNTs is higher than that of Mn–Ce/p-CNTs, which could improve the low-temperature SCR activity of NO.

The O 1s XPS spectra of the Mn–Ce/VF-CNTs catalysts were shown in Fig. 3*b*. The O 1s XPS spectra consists of two peaks assigned to the lattice oxygen at 529.5–531.3 eV and the chemisorbed oxygen at the high binding energy 531.6–532.4 eV [23]. They are denoted as O_α and O_β, respectively. The chemisorbed oxygen is from the hydroxyl groups or oxide defects. As listed in Table 2, the $O_\alpha/O_\alpha+O_\beta$ ratio over the Mn–Fe/VF-CNTs is higher than the other one. It has been demonstrated that the chemisorbed oxygen is more active than the lattice oxygen, which is ascribed to their higher mobility. Moreover, the higher O_α content could accelerate the oxidation of NO to NO_2, resulting in the subsequent facilitation of the 'fast SCR' reaction, which is beneficial to the low-temperature NH_3-SCR activity.

3.4. Catalytic activity: Fig. 4 shows the NH_3-SCR activity of the samples, as a function of the temperature within 100–300°C. It is worth noting that the NO conversion over all the catalysts increases first with the rising temperature. The maximum NO conversion rate of 88% of the Mn–Ce/p-CNTs was reached at 200°C. However, the rate of maximum NO conversion of the Mn–Ce/VF-CNTs is 99% and good catalytic performance could be maintained from 180 to 240°C. It can be seen that the Mn–Ce/ VF-CNTs catalysts has the higher NH_3-SCR activity than the catalysts synthesised by other ways. It also can be observed that the NO conversion of the CNTs without metal oxides is about 11% and we can exclude the catalysis of CNTs to the reaction. It is remarkable that the Mn–Ce/VF-CNTs demonstrated a wider operation temperature window. From the XRD and XPS results, the good dispersion degree of the active components on the Mn–Ce/VF-CNTs surface leads to enhancement of the reduction, which could increase the SCR activity. Moreover, the higher O_α contents on the catalyst surface could facilitate the 'fast SCR' process and be in favour of the excellent catalytic reduction of NO. As is well documented in the documents, the higher Mn and Mn^{4+} contents are exposed on the surface of the Mn–Ce/ VF-CNTs catalysts, which results in the more active sites for the SCR-NH_3 reaction. The interaction of MnO_x and CeO_x could promote the oxidation of NO to NO_2, which can enhance the SCR activity. Additionally, the N_2 selectivity of the catalysts is shown in Fig. 4*b* as a function of reaction temperature. As shown

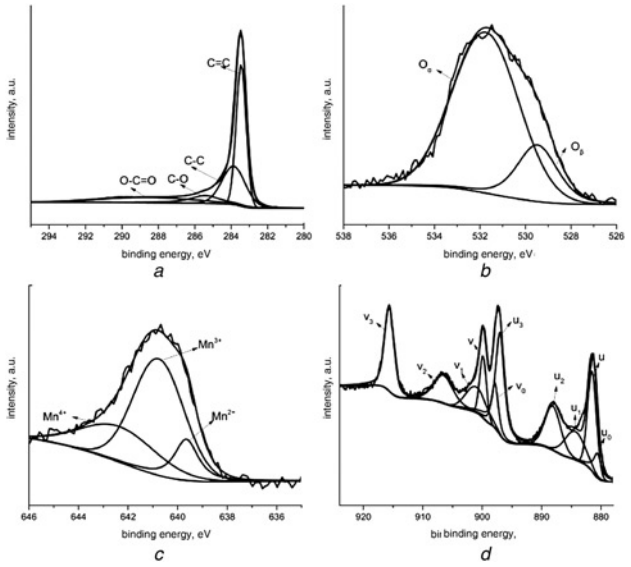

Fig. 3 *XPS spectra for*
a C 1s
b O 1s
c Mn 2p
d Ce 3d of the Mn–Ce/VF-CNTs catalysts

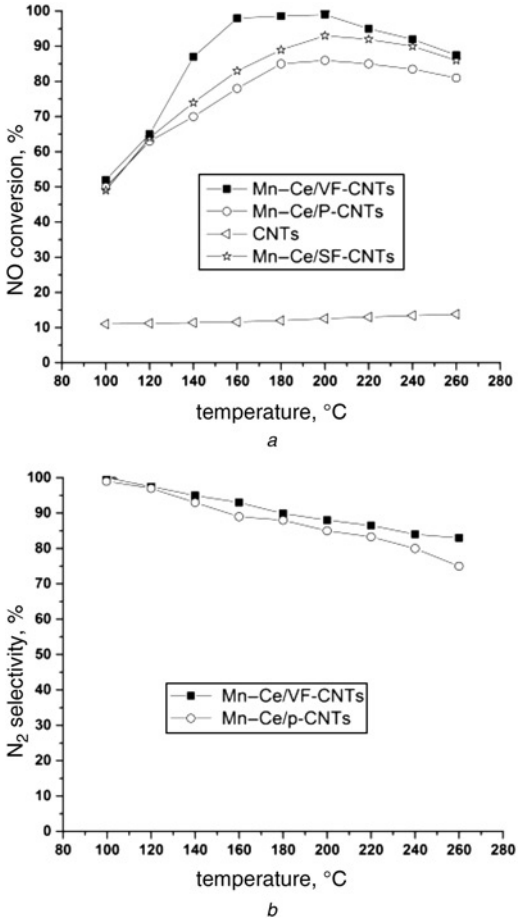

Fig. 4 *NH_3-SCR performance of Mn–Ce/VF-CNTs and Mn–Ce/p-CNTs*
a Catalytic activity
b N_2 selectivity reaction conditions: $[NO]=[NH_3]=500$ ppm, $[O_2]=5\%$, N_2 balance and GHSV = 20,000 h^{-1}

in Fig. 4*b*, the Mn–Ce/VF-CNTs catalysts are more selective for the low-temperature NH_3-SCR of NO. Generally, the Mn–Ce/VF-CNTs catalysts demonstrate highly active and selective for the low-temperature NH_3-SCR of NO_x.

4. Conclusion: In summary, we successfully developed the Mn–Ce/VF-CNTs via a facile and green method. The obtained samples enhanced NH_3-SCR activity of NO. The CNTs functioned by HNO_3 vapour could be associated with the high specific surface areas, oxygen-containing functioned groups. The high specific surface areas are beneficial for the adsorption of the reagents, leading to high catalytic activity. The oxygen-containing functioned groups could enhance the hydrophilic nature of the nanotubes surface and provide the anchoring sites for catalyst precursor complexes, which could result in the uniform distribution of active sites and be in favour of the excellent catalytic performance. Based on these favourable properties, the catalysts could possess the excellent low-temperature NH_3-SCR activity of NO.

5. Acknowledgment: This work was sponsored financially by Creative Activity Plan for Shanghai University Students (grant no. PE 2016099).

6 References

[1] Roy S., Hegde M.S., Madras G.: 'Catalysis for NO_x abatement', *Appl. Energy*, 2009, **86**, pp. 2283–2297
[2] Fang C., Zhang D.S., Cai S.X., *ET AL.*: 'Low-temperature selective catalytic reduction of NO with NH_3 over nanoflaky MnO_x on carbon nanotubes in situ prepared via a chemical bath deposition route', *Nanoscale*, 2013, **5**, pp. 9199–9207
[3] Chen Z., Yang Q., Li H., *ET AL.*: 'Cr–MnO_x mixed-oxide catalysts for selective catalytic reduction of NO_x with NH_3 at low temperature', *J. Catal.*, 2010, **276**, pp. 56–65
[4] Wang X., Zheng Y., Xu Z., *ET AL.*: 'Amorphous MnO_2 supported on carbon nanotubes as a superior catalyst for low temperature NO reduction with NH_3', *RSC Adv.*, 2013, **3**, pp. 11539–11542
[5] Shan W., Song H.: 'Catalysts for the selective catalytic reduction of NO_x with NH_3 at low temperature', *Catal. Sci. Technol.*, 2015, **5**, pp. 4280–4288
[6] Li J., Chang H., Ma L., *ET AL.*: 'Low-temperature selective catalytic reduction of NO_x with NH_3 over metal oxide and zeolite catalysts – a review', *Catal. Today*, 2011, **175**, pp. 147–156
[7] Wu Z., Jin R., Wang H., *ET AL.*: 'Effect of ceria doping on SO_2 resistance of Mn/TiO_2 for selective catalytic reduction of NO with NH_3 at low temperature', *Catal. Commun.*, 2009, **10**, pp. 935–939
[8] Cen W., Liu Y., Wu Z., *ET AL.*: 'A theoretic insight into the catalytic activity promotion of CeO_2 surfaces by Mn doping', *Phys. Chem. Chem. Phys.*, 2012, **14**, pp. 5769–5777
[9] Fan X., Qiu F., Yang H., *ET AL.*: 'Selective catalytic reduction of NO_x with ammonia over Mn–CeO_x/TiO_2-carbon nanotube composites', *Catal. Commun.*, 2011, **12**, pp. 1298–1301
[10] Beale A.M., Gao F., Lezcano-Gonzalez I., *ET AL.*: 'Recent advances in automotive catalysis for NO_x emission control by small-pore microporous materials', *Chem. Soc. Rev.*, 2015, **44**, pp. 7371–7405
[11] Samojeden B., Motak M., Grzybek T.: 'The influence of the modification of carbonaceous materials on their catalytic properties in SCR-NH_3', *C. R. Chim.*, 2015, **18**, pp. 1049–1073
[12] Hou P.X., Liu C., Cheng H.M.: 'Purification of carbon nanotubes', *Carbon*, 2008, **46**, pp. 2003–2025
[13] Kim S.W., Kim T., Kim Y.S., *ET AL.*: 'Surface modifications for the effective dispersion of carbon nanotubes in solvents and polymers', *Carbon*, 2012, **50**, pp. 3–33
[14] Ming J., Wu Y., Yu Y., *ET AL.*: 'Steaming multiwalled carbon nanotubes via acid vapour for controllable nano-engineering and the fabrication of carbon nanoflutes', *Chem. Commun.*, 2011, **47**, pp. 5223–5225
[15] Likodimos V., Steriotis T.A., Papageorgiou S.K., *ET AL.*: 'Controlled surface functionalization of multiwall carbon nanotubes by HNO_3 hydro-thermal oxidation', *Carbon*, 2014, **69**, pp. 311–326
[16] Cao Z., Qiu L., Yang Y., *ET AL.*: 'The effects of surface modifications of multiwalled carbon nanotubes on their dispersibility in different solvents and poly (ether ether ketone)', *J. Mater. Res.*, 2014, **29**, pp. 2625–2633
[17] Cabana L., Ke X., Kepić D., *ET AL.*: 'The role of steam treatment on the structure, purity and length distribution of multi-walled carbon nanotubes', *Carbon*, 2015, **93**, pp. 1059–1067
[18] Xia W., Jin C., Kundu S., *ET AL.*: 'A highly efficient gas-phase route for the oxygen functionalization of carbon nanotubes based on nitric acid vapor', *Carbon*, 2009, **47**, pp. 919–922
[19] Wang C., Sun L., Cao Q., *ET AL.*: 'Surface structure sensitivity of manganese oxides for low-temperature selective catalytic reduction of NO with NH_3', *Appl. Catal. B Environ.*, 2011, **101**, pp. 598–605
[20] Santangelo S.: 'Controlled surface functionalization of carbon nanotubes by nitric acid vapors generated from sub-azeotropic solution', *Surf. Interface Anal.*, 2016, **48**, pp. 17–25
[21] Wang X., Zheng Y., Xu Z., *ET AL.*: 'Low-temperature selective catalytic reduction of NO over MnO_x/CNTs catalysts: effect of thermal treatment condition', *Catal. Commun.*, 2014, **50**, pp. 34–37
[22] Xiao X., Sheng Z., Yang L., *ET AL.*: 'Intermetallic molybdenum carbide for pseudocapacitive electrode material', *Catal. Sci. Technol.*, 2016, **6**, pp. 1507–1514
[23] Wang L., Huang B., Su Y., *ET AL.*: 'Manganese oxides supported on multi- walled carbon nanotubes for selective catalytic reduction of NO with NH_3: catalytic activity and characterization', *Chem. Eng. J.*, 2012, **192**, pp. 232–241

doi: 10.1049/mnl.2016.0593